Presented at the Symposium on
Advanced Technology Arising from
Particle Physics Research, ANL,
Argonne, IL, May 17, 1973

LBL-2092

LIQUID XENON FILLED WIRE CHAMBERS FOR MEDICAL IMAGING APPLICATIONS

S. E. Derenzo, T. F. Budinger, R. G. Smits,
H. Zaklad, and L. W. Alvarez

May 1973

Prepared for the U. S. Atomic Energy Commission
under Contract W-7405-ENG-48

LIQUID XENON FILLED WIRE CHAMBERS FOR MEDICAL IMAGING APPLICATIONS*

S. E. Derenzo, T. F. Budinger, R. G. Smits,
H. Zaklad, and L. W. Alvarez

Lawrence Berkeley Laboratory
University of California
Berkeley, CA 94720

ABSTRACT

In 1968, Luis Alvarez suggested that a high-resolution multiwire particle detector could be developed using a thin layer of liquified noble gas as the detection medium. After key problems in chamber construction, purification, and readout had been solved, a spatial resolution of 15 μ rms was demonstrated. Work is in progress to build high-resolution chambers and measure their properties for particle physics experiments at high-energy accelerators.

The liquid xenon multiwire chamber also has potential in nuclear medicine for imaging isotope distributions with an unprecedented combination of gamma-ray detection efficiency and spatial resolution. A preliminary 24-wire chamber has been constructed; this chamber detects 280-keV gamma rays with 65% efficiency and 4-mm FWHM spatial resolution. Initial images of point and distributed sources are very promising, and the liquid purity can be maintained for periods exceeding several days.

1. INTRODUCTION

This paper outlines the development of liquid-filled wire chambers up to the present time. Although the initial motivation was high spatial resolution for particle physics experiments, other applications such as the imaging of x rays and γ rays in astrophysics and medical sciences are also appealing. This paper places particular emphasis on the use of liquid xenon multiwire gamma-ray detectors in clinical medicine for the diagnosis of human disease.

2. INITIAL MOTIVATION AND DEVELOPMENT

The gas-filled wire chamber plays an important role in particle physics, primarily because it can simultaneously provide fast electronic pulses and a spatial accuracy approaching ± 0.2 mm (0.4 mm FWHM). In 1968, Alvarez suggested that the spatial accuracy of the wire chamber could be improved ten to one-hundred fold by greatly reducing the thickness of the detecting layer and filling this layer with a liquified noble gas.[1] Such detectors would be invaluable for tracing the paths of high-energy particles through magnetic fields, whether in cosmic-ray experiments or in particle physics studies at the new multi-hundred GeV accelerators.

Previous work over the past twenty-five years had demonstrated that small chambers filled with liquid argon and liquid xenon were capable of detecting ionizing radiation by collecting the ionization electrons.[2-8] It also became known that a contamination of only a few parts per million of oxygen would poison the liquid by capturing the ionization electrons before they traveled a few mm.[9] Because of the tremendous potential of liquid-filled chambers, however, we were motivated to solve the purification, construction, and readout problems that had discouraged the development of practical devices. We began our work using simple cylindrical chambers filled with liquid argon (see Fig. 1).

Argon is the least expensive of the liquified noble gases and the easiest to handle. Initially, impurity problems were severe, as the best commercially available argon gas contained several ppm O_2 and a single pass through our early purifiers did not provide adequate purification. One day we emptied and refilled a chamber so as to pass the gas through the purifier a second time. The liquid was much cleaner, prompting us to install a circulation pump to pass the gas through the purifier thousands of times before it was liquified in the chamber. The result was liquid containing < 0.1 ppm O_2.[10]

By using a fine tungsten wire 4 μ in diameter to produce electric fields $> 10^6$ V/cm, we were able to observe amplified pulses arising from some electron avalanche process in the liquid. We were quite encouraged by this, and began to think about low-cost schemes for reading out arrays of such fine wires.[11] Unfortunately, the avalanche pulses occurred only at a few small regions scattered along the wire.[12]

Thus we turned to liquid xenon (which is a much better detection medium for the gamma rays used in nuclear medicine) and found that the electron avalanche was much better behaved than in liquid argon—the amplified pulses occurred with high reliability along the entire length of the wire. In addition, the pulses were proportional to the initial ionization, a necessary property for determining the energy of gamma rays.[13] Liquid xenon proved much more difficult to purify than liquid argon, requiring improvements in our noble gas purifier, more carefully constructed chambers, and the use of field emission electrons from the 3.5-μ wires to selectively sweep electronegative impurities from the bulk of the liquid. These measures remove nearly all of the impurities, and we seldom detect any electron capture in our chambers. Typically, the electron capture is less than 1% per mm drift in fields of a few kV/cm.

Ultimately, we learned that the electron avalanche does not readily occur on closely spaced wires, which led us to investigate the smaller ionization pulses. Using a wire spacing of 50 μ in liquid xenon, we have shown that a space resolution of 15 μ rms can be achieved for charged particles;[13] as a result we are now building small high-resolution chambers with wire spacings of 20 μ to measure their properties for high-energy physics.[14]

Using 3.5-μ wire and pure liquid xenon, single-wire chambers readily provide avalanche gains as high as 200; and due to the high density (3.06 g/cm^3) and high atomic number (54) of liquid xenon, they are conveniently tested with gamma-ray sources. Figure 2 shows the pulse height spectrum from a ^{203}Hg source obtained when the chamber of Fig. 1 is filled with pure liquid xenon. The applied potential is 2400 V and the proportional gain is 10. The 68-keV and 279-keV photopeaks are quite prominent, as is the 279-keV Compton edge (which appears at 140 keV). At this point we had a detector with high gamma-ray detection efficiency, promising energy resolution, and proportional electron multiplication to facilitate a simple readout—capabilities that appeared attractive for applications in radiology and nuclear medicine.

3. APPLICATIONS IN MEDICAL IMAGING

After discussing the merits of multiwire liquid xenon chambers with several nuclear medicine specialists at LBL's Donner Laboratory (including Thomas Budinger, Hal O. Anger, and James McRae), we designed and built a small 24-wire chamber to explore the potential of this technology in nuclear medicine.[15]

3.1. Conventional Approaches in Radiographic and Isotope Imaging in Medicine.

In order to place our detector in perspective, it will be helpful to review the conventional approaches used to image human organs:

x-radiography, rectilinear radioisotope scanning, and scintillation camera imaging.

X-radiography is the classical clinical procedure in which a beam of x-rays is selectively absorbed by features within the patient. The transmitted x-rays interact in an intensifier (photon converter) screen and record their presence on photographic film. The resulting images have excellent resolution; but contrast suffers from the fact that soft tissues, such as the heart, kidney, liver, brain, etc., are of nearly uniform density and cannot be easily distinguished from body fluids or from surrounding tissues such as muscle or fat. Of course, good anatomical information is obtained for these soft tissues if they are contiguous to bone, air, or lung. Injected dyes containing high-Z materials (barium or iodine) are used to trace blood vessels, heart chambers, and kidney function by following the movement of the injected dye on successive radiographic images.

Decades ago, it was discovered that many organs preferentially absorb certain chemicals labeled with gamma-ray-emitting isotopes, causing the organ to "glow" from within. The absorption of iodine by the thyroid is a good example. A lead collimator is used to select gamma rays originating only from a small region within the patient. These gamma rays can then be detected by a single-crystal NaI (Tl) scintillator-photomultiplier combination. This assembly is systematically "scanned" back and forth across the area of interest so that by recording the number of gamma rays detected at each point, one can construct a map of the activity. It is important to realize that this technique not only allows organs to be imaged with a contrast not otherwise available, it also allows organ function to be visualized because the absorption of the labeled chemical is often abnormal in regions where organ function is abnormal.

This procedure was revolutionized in the late 1950's when Hal Anger developed the scintillation camera at LBL's Donner Laboratory.[16] This device consists of a single-crystal of NaI (Tl) scintillator of larger area than the scanner detector (typically 12-in. diameter and 1/2-in. thick) viewed by an array of photomultipliers. A pinhole or multichannel lead collimator is placed in front of one face of the crystal so that the gamma rays emanating from each point in the patient can interact only in a very limited region of the crystal. The X and Y coordinates of the center of intensity of the scintillation light from each interacting gamma ray are determined by suitable electronics, and this position information is used to produce a single dot on a cathode ray tube display.

A picture of the isotope distribution is made up of many such dots. The scintillation camera has a resolution of typically 9 mm FWHM at 140 keV and approximately 6 mm FWHM at 511 keV.[16] This camera simultaneously records gamma rays from the entire area of interest and is much faster than the rectilinear scanner. Data rates in excess of 50,000 events per sec can give a picture every 0.1 sec, permitting "motion picture" photography of blood flow through the heart and lung spaces.

A promising new type of gamma camera—the solid state camera—was recently evaluated.[17] By cutting grooves in the anode and the cathode of a large lithium-drifted germanium crystal (4.4 cm), McCready et al. achieved both good spatial resolution (~ 3 mm FWHM) and excellent energy resolution (~ 1% FWHM at 140 keV). However, several problems were encountered: high cost of the germanium detector, limited size of available crystals, lack of detection uniformity, and variations with time. These difficulties must be solved to make a useful camera.

3.2. Liquid Xenon Multiwire Gamma Ray Camera

The liquid xenon multiwire gamma ray camera we are developing uses a lead collimator in the same manner as the scintillation camera but detects the gamma ray somewhat differently (see Fig. 3). Rather than using the flash of scintillation light, we use the electrons liberated by the interacting gamma rays. These electrons can be transported with high efficiency over distances of many cm in sufficiently pure liquid xenon, and are attracted to the nearest anode wire where they avalanche to produce the desired electrical signals. This detector is similar to the gas-filled multiwire proportional chamber, except that the wires are much finer and the gas filling is replaced with very pure liquid xenon. In this context, it is interesting to compare the photopeak efficiency of liquid xenon with that of gaseous xenon at 1 and 10 atm (see Fig. 4). We see that pressurized xenon-filled wire chambers[18] are quite useful for photons of energy $\leq$ 80 keV but have very low efficiency for the 140- to 511-keV gamma rays now used in nuclear medicine. A 2.5-cm thick chamber pressurized with xenon gas at 10 atm has a photopeak efficiency of only 9% at 140 keV and 0.3% at 511 keV. The corresponding figures for liquid xenon are 100% and 36%.

In order to maintain the required degree of purity, our chambers are constructed of only ceramic, glass, and metal. Figure 5 shows a piece of ceramic that serves both as a pressure window and the supporting member for the electrodes. Twenty-four 3.5-μ wires are stretched across and spot welded to pairs of kovar pins. The pins are sealed to the ceramic with glass and protrude from the other side where the electronic readout is attached. The wide strips below the wires (and orthogonal to them) provide the orthogonal coordinate from the pulse induced by each avalanche. The liquid xenon layer is 2-cm

thick and the photopeak detection efficiency for 279-keV gamma rays is 65%. The liquid purity has been maintained for periods as long as 5 days. (For further details see ref. 19).

Tests of the resolution and contrast capabilities of our camera have thus far included moving point sources and an emission pattern in the shape of the letters "XE". Slots were cut in a 1-in. lead block to aim back toward a single point so that a small ^{203}Hg source (279-keV gamma rays) could produce the desired distribution. A comparison of images from our 24-wire liquid xenon chamber (left) and the 12-in. diameter scintillation camera at LBL's Donner Laboratory (right) is shown in Fig. 6. This preliminary comparison shows that the wire chamber has the expected 2- to 3-fold improvement in resolution.

3.3. Limitations Imposed by the Collimator

In a clinical situation, an increase in resolution requires an increase in the number of initial gamma rays because the transmission of the collimator is proportional to the square of the resolution. A collimator having a resolution of 3 mm (to match our liquid xenon wire chamber) unfortunately has a transmission 10 times smaller than that of the 10-mm collimators in common use. However, in many situations it is reasonable to increase both the administered activity and the exposure time. These include studies involving the short-lived isotopes 13-hr ^{123}I, 6-hr ^{99m}Tc, 1.67-hr ^{113m}In (from 115-day ^{113}Sn), 66-sec ^{82}Rb (from 25-day ^{82}Sr), 13 sec ^{81m}Kr (from 4.7-hr ^{81}Rb), 20-min ^{11}C, 10-min ^{13}N, and 2.1-min ^{15}O.

3.4. Positron Coincidence Imaging

Is there any way to overcome the limitations in sensitivity associated with the collimator? There is! For the past twenty years, experimental cameras have been built to image isotopes that decay by

positron emission.[16,20] These cameras consist of two detectors in time coincidence, one located on either side of the patient. The positron is an antielectron; and when it comes to rest in tissue or other matter, it annihilates with a nearby electron to simultaneously produce two 511-keV gamma rays that fly outward in opposite directions. By detecting the two gamma rays in coincidence, one can measure their flight direction rather than select only a small range of directions as a collimator does. The result is a camera with unparalleled sensitivity and a spatial resolution limited by the detector and to some extent by the range of the positrons in tissue.

When the scintillation camera is used in this mode, the spatial resolution is typically 6 to 10 mm FWHM; but the maximum data rate is only 1000 counts per sec. This is basically limited by the time resolution of the camera and the resulting rate of "accidental coincidences." By using two matrices of NaI (Tl) crystals, Brownell and co-workers have achieved counting rates of 50,000 per sec and a spatial resolution of 10 mm FWHM.[21]

Liquid xenon wire chambers do not at first sight appear suitable for positron coincidence imaging because the slow drift speed of the electrons (3×10^5 cm/sec) limits the time resolution to typically 5 to 10 μsec. Liquid xenon is a very fast (< 10^{-9} sec) scintillator, however;[22] and this light can be used to provide a prompt timing signal while anode-cathode arrays provide accurate position information. The result could be a positron camera with a data rate of 5,000 to 10,000 counts per sec and a potential space resolution of 1 mm FWHM.[23]

In summary, the high sensitivity of the positron coincidence camera is offset in most schemes by rate limitations that can be more severe than the sensitivity limitations of a collimated gamma camera.

3.5. Image Contrast and Energy Resolution

Image contrast is as important as resolution and efficiency in determining the value of an imaging procedure in nuclear medicine. Even if the isotope is well localized, some of the gamma rays scatter in the tissue of the patient; and these will seriously degrade image contrast if they are not rejected by the imaging system. In scattering, the gamma rays lose varying amounts of energy, the energy lost being smaller for smaller scattering angles; thus the ability to reduce the effects of scattering depends critically on the energy resolution of the detector.[24] The liquid xenon multiwire proportional chamber has a pulse-height spread of 20 to 30% FWHM, mostly due to variations in electric field along the wires. This is about twice the energy spread of the NaI (Tl) scintillation camera.

It is possible to build a liquid xenon wire chamber with far better energy resolution. Working in the ionization mode (rather than the proportional avalanche mode) gives pulses that are far smaller; but modern low-noise field-effect transistors can handle these signals and introduce much less pulse-height spread than does electron amplification in the liquid itself. Other factors, such as electron statistics, are also small. We hope ultimately to achieve 5% FWHM at 140 keV and 2% FWHM at 511 keV. To explore these limitations, we constructed a simple three-electrode ionization chamber containing a "Frisch grid" to reduce the variation in pulse height due to the variation in gamma-ray interaction points (see Fig. 7). A collimated beam of 279-keV gamma rays was sent into this chamber, with a resulting energy resolution of 10% FWHM—slightly better than NaI (Tl) (see Fig. 8) but below our expectations. Work in this area continues.

4. CONCLUSION

We conclude on the optimistic note that the liquid xenon detector technology is steadily expanding toward important applications in both particle physics and nuclear medicine.

ACKNOWLEDGMENTS

We are indebted to Joseph Savignano, Tony Vuletich, and Buck Buckingham for their skill and patience in building and maintaining our equipment. We thank Gary Chanan for assistance in data-taking and are grateful to H. O. Anger and Richard Muller for many helpful discussions.

FOOTNOTE AND REFERENCES

*Work done under the auspices of the U. S. Atomic Energy Commission.

1. L. W. Alvarez, Lawrence Radiation Laboratory, Group A Physics Note No. 672, 1968 (unpublished).

2. N. Davidson and A. E. Larsh, Jr., Phys. Rev. 74, 220 (1948); 77, 706 (1950).

3. G. W. Hutchinson, Nature 162, 610 (1948); thesis, St. John's College, Cambridge, 1951 (unpublished).

4. A. N. Gerritsen, Physica 14, 407 (1948).

5. M. S. Malkin and H. L. Schultz, Phys. Rev. 83, 1051 (1951).

6. John Marshall, Rev. Sci. Instr. 25, 232 (1954).

7. D. W. Swan, Proc. Phys. Soc. 76, 36 (1960).

8. H. D. Pruett and H. P. Broida, Phys. Rev. 164, 1138 (1967).

9. The most carefully studied case is that of oxygen in liquid argon: D. W. Swan, Proc. Phys. Soc. 83, 659 (1964). Swan found that the number of free electrons N(X) surviving after drifting a distance X was given by

$$N(X) = N(0)\, e^{-8XC/E}$$

where X is in cm, C is the oxygen concentration in ppm, and E is the electric field in kV/cm.

10. Haim Zaklad (D. Eng. thesis), Lawrence Radiation Laboratory Report UCRL-20690 (1971).

11. S. E. Derenzo, R. A. Muller, R. G. Smits, and L. W. Alvarez, Lawrence Radiation Laboratory Report UCRL-19254 (1969); same as National Accelerator Laboratory, 1969 Summer Study Report SS-154, Vol. III, p. 79.

12. S. E. Derenzo, D. B. Smith, R. G. Smits, H. Zaklad, L. W. Alvarez, and R. A. Muller, Lawrence Radiation Laboratory Report UCRL-20118; same as National Accelerator Laboratory, 1970 Summer Study Report SS-181.

13. R. A. Muller, S. E. Derenzo, G. Smadja, D. B. Smith, R. G. Smits, H. Zaklad, and L. W. Alvarez, Phys. Rev. Letters 27, 532 (1971).

14. S. E. Derenzo, A. Schwemin, R. G. Smits, H. Zaklad, and L. W. Alvarez, Lawrence Berkeley Laboratory Report LBL-1791, to be published in Proceedings of the 1973 International Conference on Instrumentation for High Energy Physics, May 1973. Frascati, Italy.

15. H. Zaklad, S. E. Derenzo, R. A. Muller, G. Smadja, R. G. Smits, and L. W. Alvarez, IEEE Trans. Nuclear Science, NS-19(3), 206 (1972).

16. H. O. Anger, ISA Transactions 5, 311 (1966).

17. V. R. McCready, R. P. Parker, E. M. Gunnersen, R. Ellis, E. Moss, W. G. Gore, and J. Bell, British Journal of Radiology 44, 58 (1971).

18. L. Kaufman, V. Perez-Mendez, and G. Stoker, IEEE Trans. Nucl. Sci. NS-20(1), 426 (1973); R. St. Onge, IEEE Trans. Nucl. Sci.

NS-20(1), 333 (1973); C. J. Borkowski and M. K. Kopp, IEEE Trans. Nucl. Sci. NS-19(3), 161 (1972).

19. H. Zaklad, S. E. Derenzo, R. A. Muller, and R. G. Smits, IEEE Trans. Nucl. Sci. NS-20(1), 429 (1973).

20. G. L. Brownell and W. H. Sweet, Nucleonics 11 (11), 40 (1953).

21. C. A. Burnham and G. L. Brownell, IEEE Trans. Nucl. Sci. NS-19 (3), 201 (1972).

22. J. A. Northrop, J. M. Gursky, and A. E. Johnsrud, I. R. E. Trans. Nucl. Sci. NS-5 (3), 81 (1958).

23. It is even plausable that a time resolution of ± 0.1 nsec could be realized and the difference in arrival times between the two gamma rays used to provide coarse (± 2 cm) "depth" coordinate information. This can be quite useful, as it allows the isotope distribution to be directly recorded in the form of several high resolution planar images, each corresponding to a "slice" in depth.

24. For a quantitative study of this problem, see M. M. Dresser and G. F. Knoll, IEEE Trans. Nucl. Sci. NS-20 (1), 266 (1973) and Jorge Llacer, IEEE Trans. Nucl. Sci. NS-20(1), 273 (1973). Also note that if the image contrast is low, a large number of dots must be accumulated in order that the image have sufficiently "accurate" shades of gray. For example, due to statistical fluctuations at least several hundred dots are required to reliably see a 10% variation in intensity between two areas. Only one-tenth as many dots are required to see a 30% variation in intensity.

FIGURE CAPTIONS

Fig. 1. Liquid xenon single-wire proportional chamber. Central wire is typically 3.5-μ diameter tungsten.

Fig. 2. Pulse-height spectrum from chamber of Fig. 1, showing 68-keV photopeak, 279-keV Compton edge, and 279-keV photopeak (^{203}Hg source). Proportional gain in the liquid was 10.

Fig. 3. Schematic of liquid xenon radioisotope camera under development. The gamma rays produce recoil electrons in the liquid xenon, and the resulting ionization is collected (and multiplied) on the 4-μ diameter anode wires. Two-dimensional imaging is achieved by reading the induced pulse off an array of cathode strips perpendicular to the anode wires. Liquid xenon temperature is maintained by a freon-11 bath and a liquid nitrogen heat exchanger.

Fig. 4. Photopeak efficiency as a function of gamma-ray energy for 2.5-cm layers of gaseous xenon (at 1 and 10 atm) and liquid xenon.

Fig. 5. Ceramic electrode assembly of liquid xenon multiwire chamber. Anode wires (5-μ diam.) and cathode strips are spaced 2.8 mm apart. Wires are centrally supported by passing them between two quartz fibers.

Fig. 6. Comparison of images of the letters "XE" (produced by 279-keV gamma rays) from the liquid xenon multiwire chamber (left) and the scintillation camera (right).

Fig. 7. Liquid xenon ionization chamber with Frisch grid and collimated gamma-ray source built to investigate energy resolution.

Fig. 8. Pulse-height spectrum for 279-keV gamma rays seen in setup of Fig. 7. FWHM is 10%, comparable to NaI (Tl).

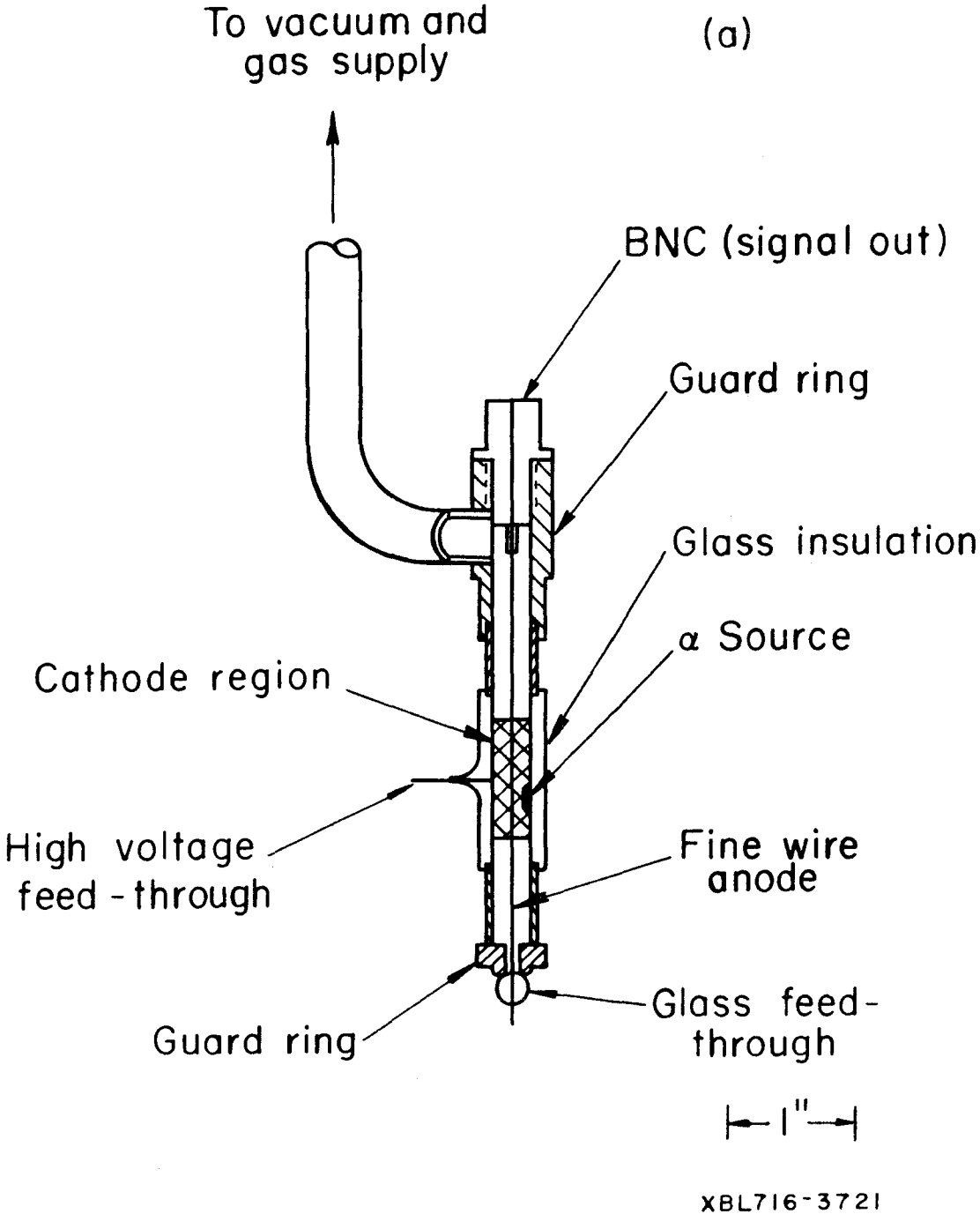
To vacuum and gas supply
(a)
BNC (signal out)
Guard ring
Glass insulation
α Source
Cathode region
High voltage feed - through
Fine wire anode
Guard ring
Glass feed - through
1"
XBL716-3721

Fig. 1

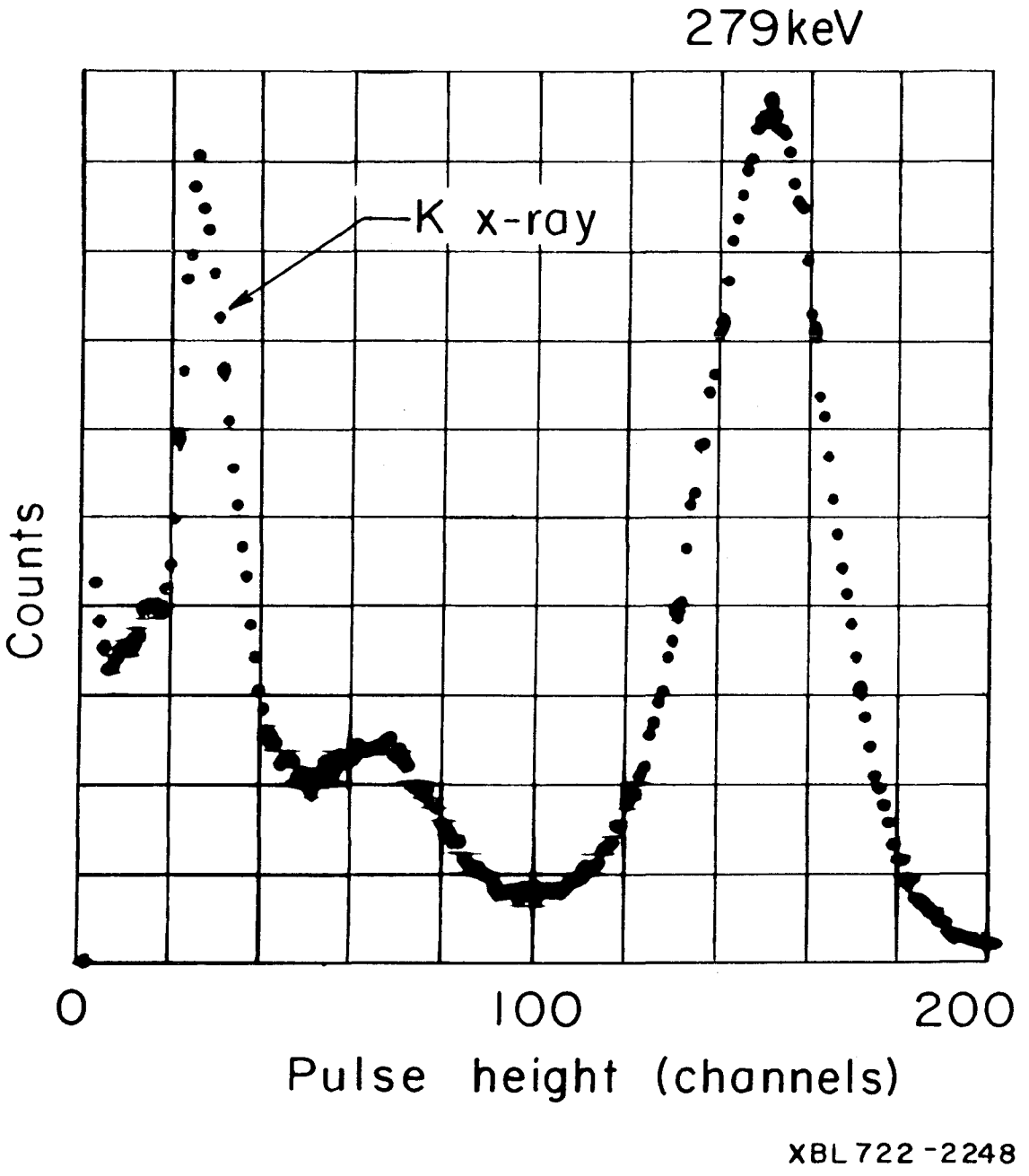
279keV
K x-ray
Counts
0
100
200
Pulse height (channels)
XBL 722-2248

Fig. 2

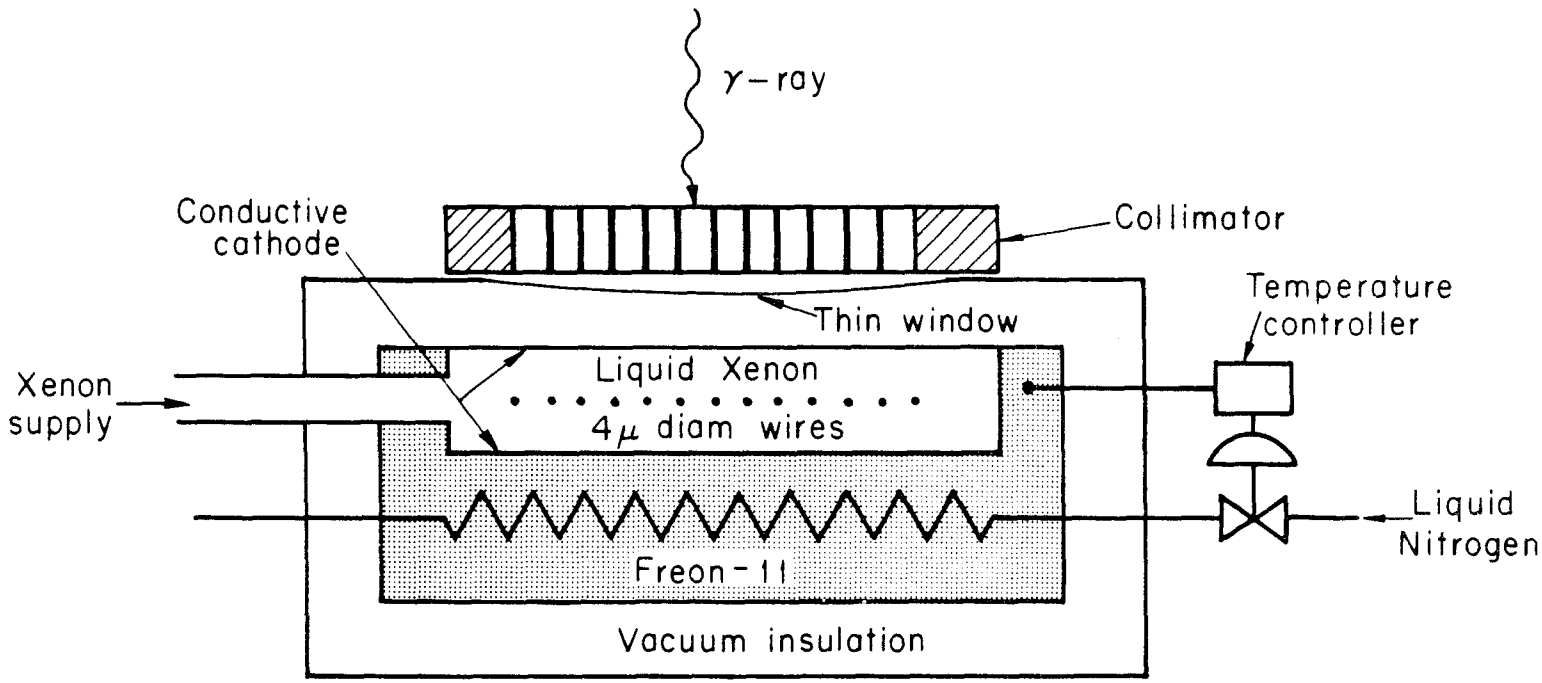
γ-ray
Conductive cathode
Collimator
Thin window
Temperature controller
Xenon supply
Liquid Xenon
4μ diam wires
Liquid Nitrogen
Freon-11
Vacuum insulation
XBL722-2348

Fig. 3

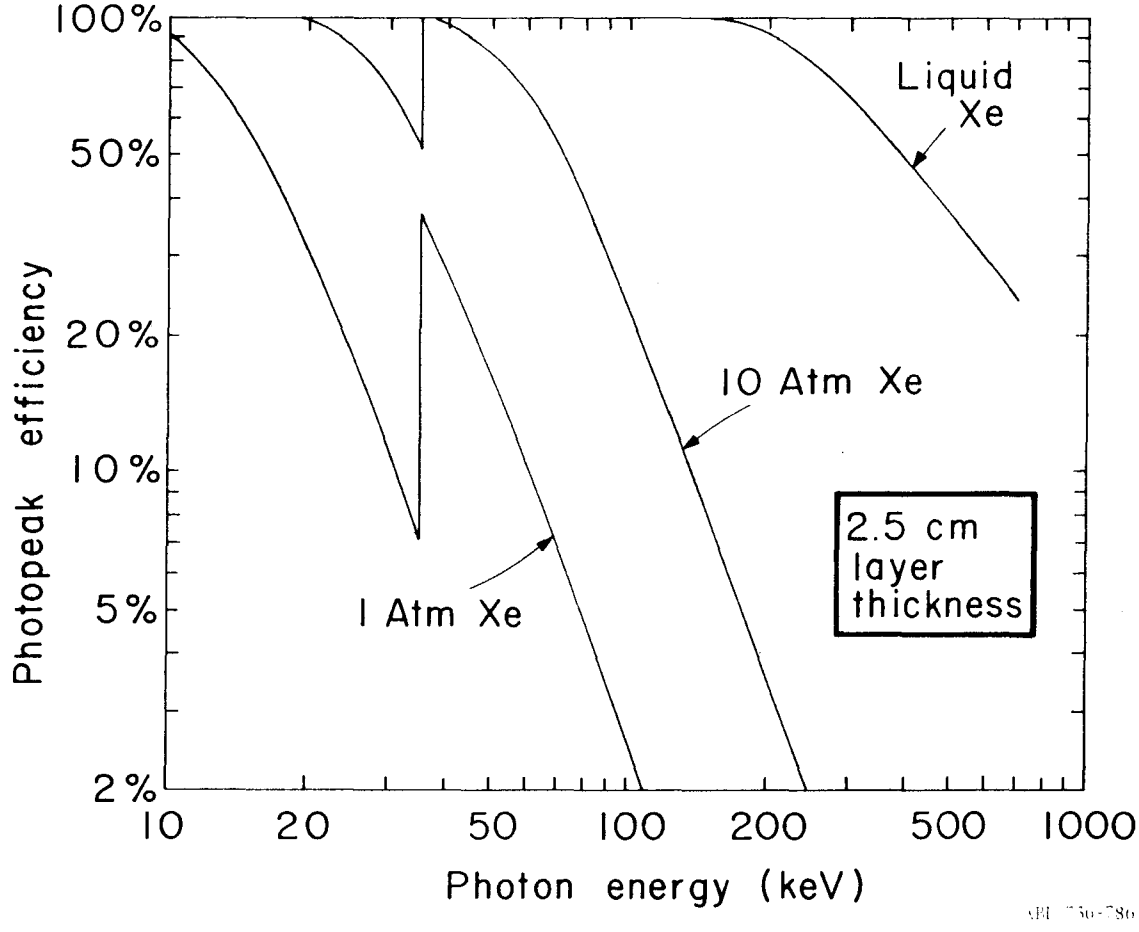
100%
50%
20%
10%
5%
2%
Photopeak efficiency
10
20
50
100
200
500
1000
Photon energy (keV)
Liquid Xe
10 Atm Xe
1 Atm Xe
2.5 cm layer thickness

Fig. 4

CBB 729-4305

Fig. 5

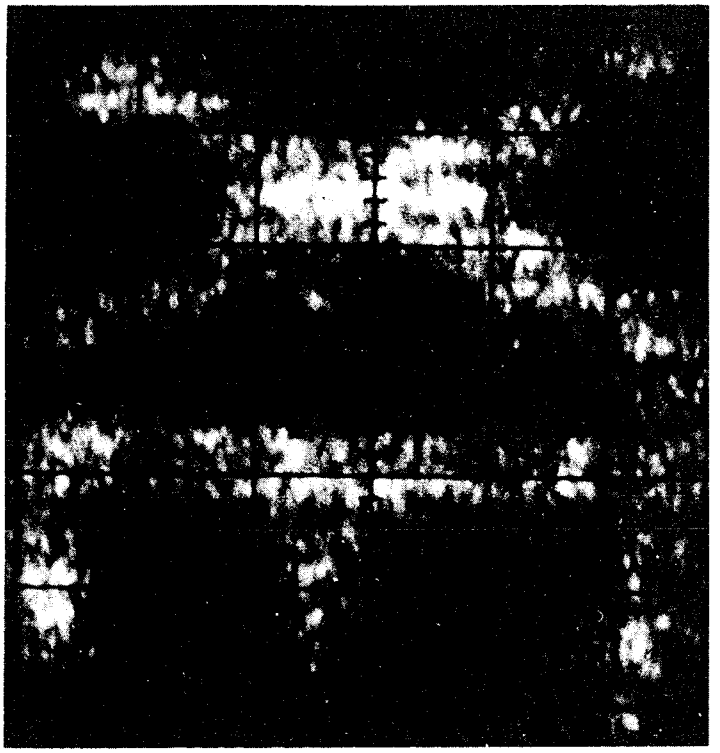

4.5 cm
(At Detector)

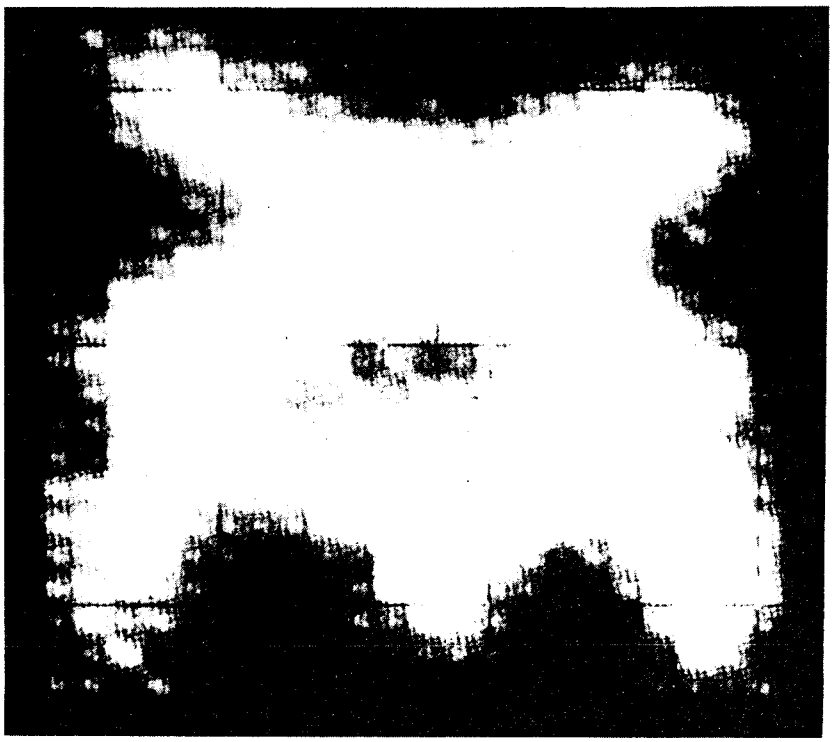

XBB 734-2780

Fig. 6

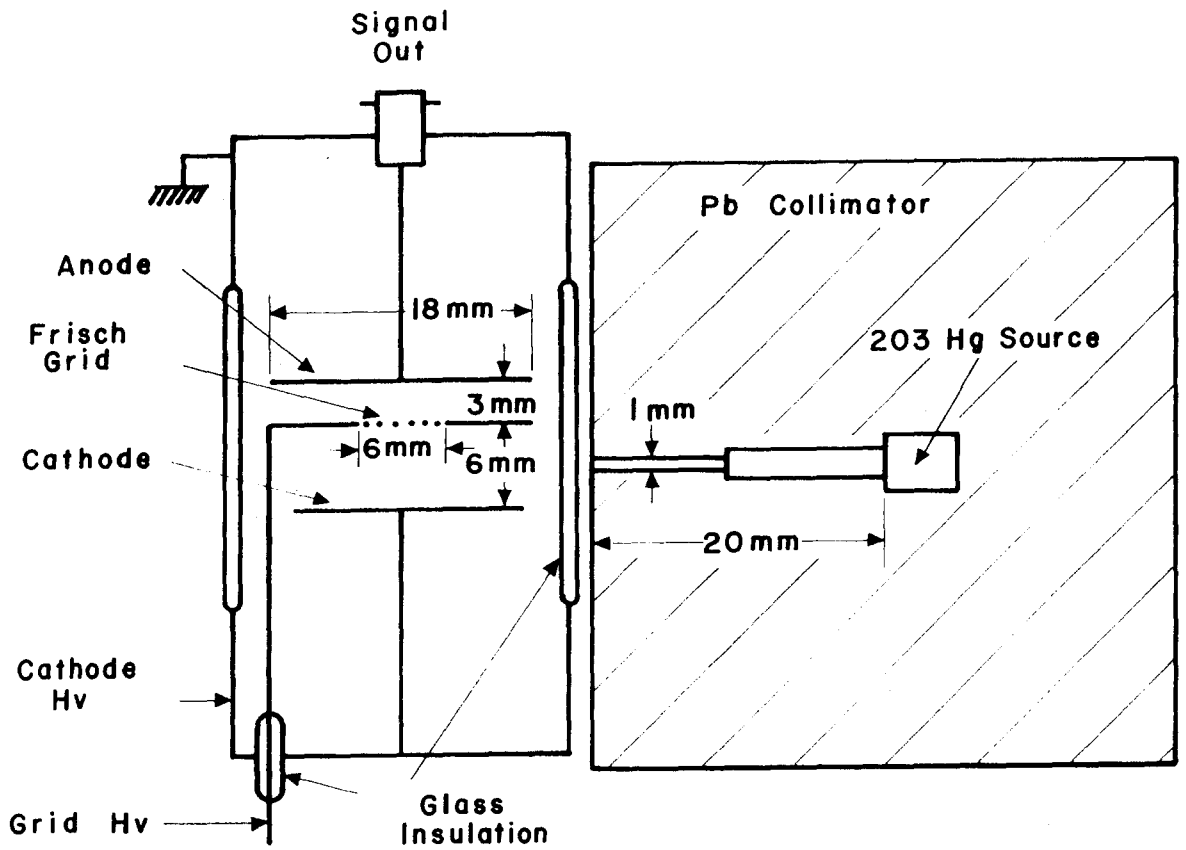
Signal
Out
Anode
Frisch
Grid
Cathode
Cathode
Hv
Grid Hv
18 mm
3 mm
6 mm
6 mm
Glass
Insulation
Pb Collimator
203 Hg Source
1 mm
20 mm
XBL 724-720

Fig. 7

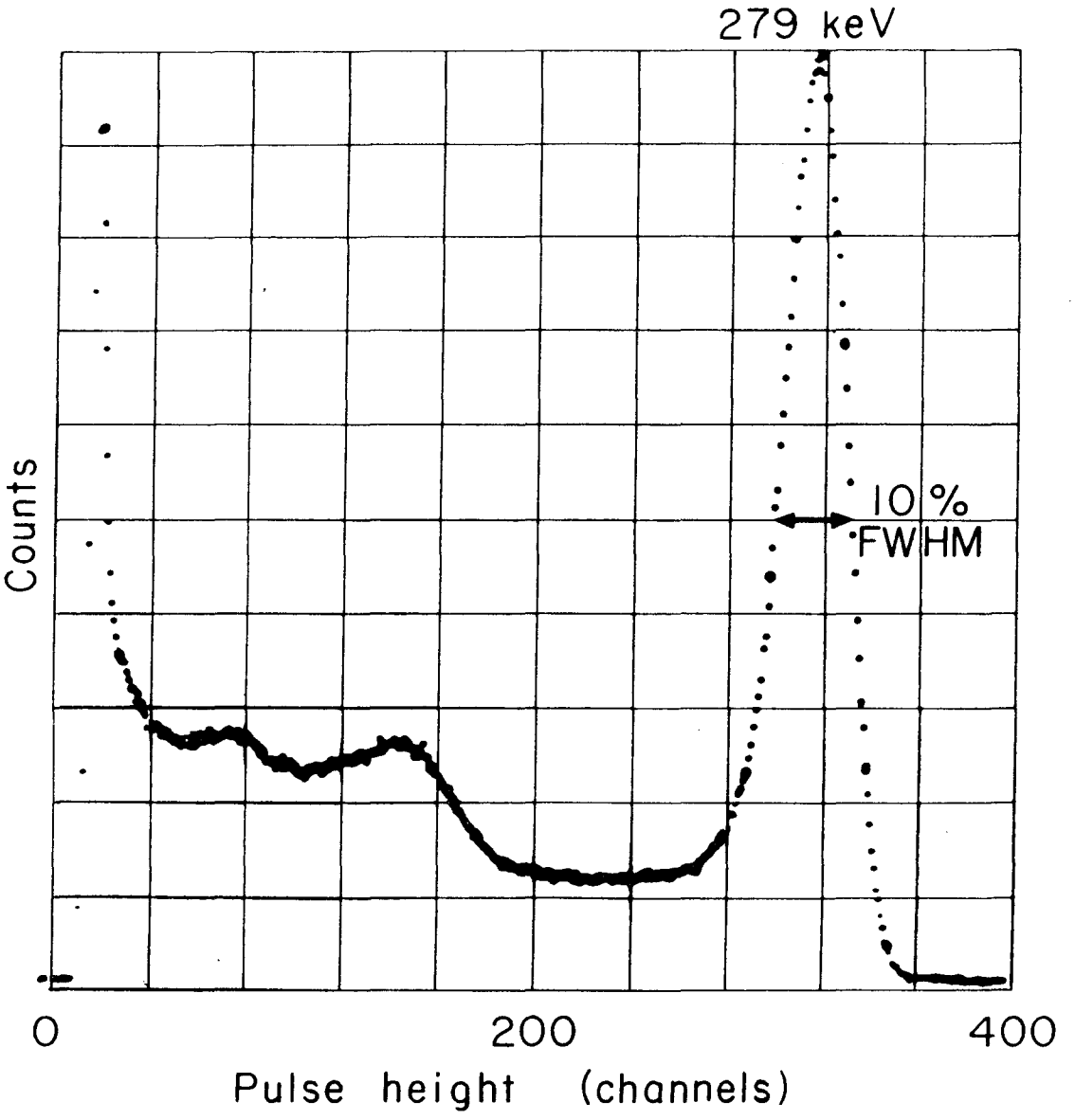

Fig. 8